J|A|C|S
ARTICLES
Published on Web 08/22/2002

A Density Functional Study of O−O Bond Cleavage for a Biomimetic Non-Heme Iron Complex Demonstrating an Fe^{V}-Intermediate

Arianna Bassan,*,† Margareta R. A. Blomberg,† Per E. M. Siegbahn,† and Lawrence Que, Jr.‡

Contribution from the Department of Physics, Stockholm Center for Physics, Astronomy and Biotechnology, Stockholm University, S-106 91, Stockholm, Sweden, and Department of Chemistry and Center for Metals in Biocatalysis, University of Minnesota, Minneapolis, Minnesota 55455

Abstract: Density functional theory using the B3LYP hybrid functional has been employed to investigate the reactivity of Fe(TPA) complexes (TPA = tris(2-pyridylmethyl)amine), which are known to catalyze stereospecific hydrocarbon oxidation when H_2O_2 is used as oxidant. The reaction pathway leading to O−O bond heterolysis in the active catalytic species Fe^{III}(TPA)−OOH has been explored, and it is shown that a high-valent iron-oxo intermediate is formed, where an Fe^{V} oxidation state is attained, in agreement with previous suggestions based on experiments. In contrast to the analogous intermediate $[(Por^{\bullet})Fe^{IV}{=}O]^{+1}$ in P450, the TPA ligand is not oxidized, and the electrons are extracted almost exclusively from the mononuclear iron center. The corresponding homolytic O−O bond cleavage, yielding the two oxidants Fe^{IV}=O and the OH· radical, has also been considered, and it is shown that this pathway is inaccessible in the hydrocarbon oxidation reaction with Fe(TPA) and hydrogen peroxide. Investigations have also been performed for the O−O cleavage in the Fe^{III}(TPA)−alkylperoxide species. In this case, the barrier for O−O homolysis is found to be slightly lower, leading to loss of stereospecificity and supporting the experimental conclusion that this is the preferred pathway for alkylperoxide oxidants. The difference between hydroperoxide and alkylperoxide as oxidant derives from the higher O−O bond strength for hydrogen peroxide (by 8.0 kcal/mol).

I. Introduction

Understanding how dioxygen is activated by metalloenzymes for the oxidation of hydrocarbons is a very active field of research in bioinorganic chemistry. Nature has evolved a number of iron enzymes, such as cytochrome P450, methane monooxygenase, and Rieske dioxygenases, that carry out highly stereoselective alkane hydroxylation, olefin epoxidation, and arene *cis*-dihydroxylation reactions.[1−4] High-valent iron-oxo species have been proposed as key intermediates in these biological oxidations. For heme enzymes such as cytochrome P450, it is generally accepted that the reactive intermediate is best described as a $[(Por^{\bullet})Fe^{IV}{=}O]^{+1}$ species,[1,5] although there is substantial discussion in the literature regarding the participation of an Fe^{III}−OOH species as a possible second oxidant.[6] On the other hand, for methane monooxygenase which has a non-heme diiron active site, the reactive species is proposed to be an $Fe_2^{IV}(\mu\text{-O})_2$ species.[7] For both of these enzymes, the key oxidizing species is formally Fe^{V}, and the two oxidizing equivalents implied by this high-valent oxidation state are delocalized over two redox-active centers, that is, the metal center and the porphyrin ligand in the former and the two iron centers in the latter. For Rieske dioxygenases, dioxygen activation is proposed to follow the heme paradigm[2,8] but must occur at a mononuclear non-heme iron center coordinated to two histidines and an aspartate.[9] This raises the question of whether a formally Fe^{V} oxidation state can be attained at a mononuclear iron center in the absence of a porphyrin ligand.

In the course of developing functional models for nonheme iron oxygenases, interesting catalytic activity was discovered for a family of nonheme iron complexes represented by $[Fe^{II}(TPA)(CH_3CN)_2]^{2+}$, where TPA is the tetradentate tripodal tris(2-pyridylmethyl)amine ligand. These catalysts utilize H_2O_2 to carry out highly stereoselective alkane hydroxylation, olefin

* To whom correspondence should be addressed. Telephone: +46 8 55378707. Fax: +46 8 55378601. E-mail: arianna@physto.se.
† Stockholm University.
‡ University of Minnesota.

(1) Sono, M.; Roach, M. P.; Coulter, E. D.; Dawson, J. H. *Chem. Rev.* **1996**, *96*, 2841−2887.
(2) Que, L., Jr.; Ho, R. Y. N. *Chem. Rev.* **1996**, *96*, 2607−2624.
(3) Solomon, E. I.; Brunold, T. C.; Davis, M. I.; Kemsley, J. N.; Lee, S.-K.; Lehnert, N.; Neese, F.; Skulan, A. J.; Yang, Y.-S.; Zhou, J. *Chem. Rev.* **2000**, *100*, 235−349.
(4) Merkx, M.; Kopp, D. A.; Sazinsky, M. H.; Blazyk, J. L.; Müller, J.; Lippard, S. J. *Angew. Chem., Int. Ed.* **2001**, *40*, 2782−2807.
(5) Schlichting, I.; Berendzen, J.; Chu, K.; Stock, A. M.; Maves, S. A.; Benson, D. E.; Sweet, R. M.; Ringe, D.; Petsko, G. A.; Sligar, S. G. *Science* **2000**, *287*, 1615−1622.
(6) For a recent discussion of a possible second oxidant in the cytochrome P450 mechanism: Ogliaro, F.; de Visser, S. P.; Cohen, S.; Sharma, P. K.; Shaik, S. *J. Am. Chem. Soc.* **2002**, *124*, 2806−2817 and references therein.
(7) Shu, L.; Nesheim, J. C.; Kauffmann, K.; Münck, E.; Lipscomb, J. D.; Que, L., Jr. *Science* **1997**, *275*, 515−518.
(8) Wolfe, M. D.; Parales, J. V.; Gibson, D. T.; Lipscomb, J. D. *J. Biol. Chem.* **2001**, *276*, 1945−1953.
(9) Kauppi, B.; Lee, K.; Carredano, E.; Parales, R. E.; Gibson, D. T.; Eklund, H.; Ramaswamy, S. *Structure* **1998**, *6*, 571−586.

10.1021/ja026488g CCC: $22.00

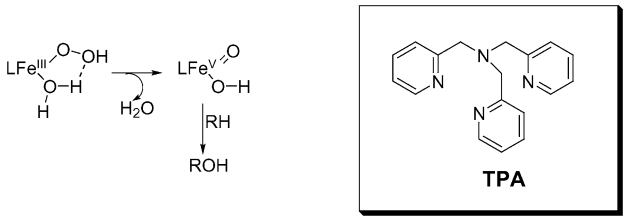

Figure 1. Proposed mechanism for hydrocarbon oxidation by $[Fe^{II}(TPA)(CH_3CN)_2]^{2+}$.

epoxidation, and olefin *cis*-dihydroxylation.[10−12] The high stereoselectivity of the oxidations excludes the involvement of HO· in the reaction mechanisms and implicates instead a more selective metal-based oxidant such as an Fe^{III}−OOH intermediate or the Fe^{V}═O species derived therefrom. The observed incorporation of ^{18}O from added $H_2^{18}O$ into oxidation products requires the involvement of an oxidant capable of solvent water exchange, such as a high-valent iron-oxo species. While the labeling results do not necessarily exclude the direct participation of the Fe^{III}−OOH intermediate in alkane hydroxylation and olefin epoxidation,[10,11] the labeling results for *cis*-dihydroxylation argue compellingly for the sole participation of an Fe^{V}═O oxidant. In the latter case, the *cis*-diol product shows nearly stoichiometric incorporation of one atom of oxygen from water and the other atom of oxygen from H_2O_2.[11,12] The proposed mechanism for forming this oxidant is illustrated in Figure 1. Before the actual hydrocarbon oxidation step, an Fe^{III}(TPA)−OOH intermediate is generated from the reaction of the Fe^{II}(TPA) complex with H_2O_2. Solvent water then binds to the Fe^{III}−OOH species to promote the heterolytic cleavage of the O−O bond. Consequent loss of water generates the *cis*-HO−Fe^{V}═O species that is proposed to be responsible for the hydrocarbon oxidations observed. The goal of the present theoretical study is to elucidate the role of the non-heme iron center in catalysis and to test the viability of an Fe^{V}═O oxidant in a TPA ligand environment as proposed in Figure 1. A low energy pathway for the conversion of the low-spin Fe^{III}−OOH intermediate to the *cis*-HO−Fe^{V}═O oxidant is found. The heterolysis of the Fe^{III}−OOH species is contrasted with the reactivity of the corresponding Fe^{III}−OO−alkyl intermediate, which has been experimentally shown to undergo O−O bond homolysis.[13,14]

II. Computational Details

The present theoretical investigation has been carried out employing density functional theory (DFT) with the B3LYP functional,[15] which includes the Becke three parameter exchange[16] and the Lee, Yang, and Parr correlation.[17]

The main quantum chemical program used is Jaguar 4.0,[18] but the Gaussian 98[19] program was employed to compute molecular Hessians (second derivatives of the energy with respect to the nuclear coordinates). Because an explicit Hessian is needed in saddle point optimizations, the geometry of the transition state was also determined using the Gaussian 98 program. Iron is described by an effective core potential (ECP),[20] and, in the geometry optimizations, all of the other atoms are described by a standard double-ζ basis set, labeled *lacvp* in Jaguar and *lanl2dz* in Gaussian. Evaluations of the Hessians were performed with the *lanl2dz* basis set. By optimizing one minimum with both basis sets, we checked that the two different basis sets, *lacvp* and *lanl2dz*, give very similar structures and energies. The resulting energy difference, computed with one of the double-ζ basis sets for the two differently optimized structures, is about one-half of a kcal/mol. The final B3LYP energies for the fully optimized structures were computed using a large basis set with polarization functions on all atoms (labeled *lacv3p*** in Jaguar).[18] The energies reported are free energies, including zero-point and thermal effects (T = 298.15 K).

Long-range solvent effects were evaluated in the present theoretical investigation by modeling the solvent as a macroscopic continuum with dielectric constant ϵ and the solute contained in a cavity of this continuous medium. Specifically, the cosmo model as implemented in Gaussian 98 was used,[21] where the dielectric constant of acetonitrile (ϵ = 36.64) was chosen according to the conditions adopted in the experiments. The dielectric medium has very small effect on the energetics of the transition states, as expected for the present type of reactions.[22,23]

The performance of the B3LYP method has been investigated using the G2 benchmark tests on a reference set of molecular properties for small first- and second-row molecules showing that hybrid DFT methods perform almost as well as the G2 method.[24,25] The B3LYP method becomes a bit less accurate when transition metals are involved[23] or when transition states are computed. An overall average error of 3−5 kcal/mol is expected for the computed energetics of the present system.

III. Results and Discussion

Quantum mechanical calculations have been performed to shed light on the O−O bond heterolytic cleavage step shown in Figure 1, proposed previously for Fe^{III}(TPA)−OOH complexes on the basis of experimental observations.[10] Because experiments have shown that in the analogous Fe^{III}(TPA)−alkylperoxide complexes, the O−O bond is instead cleaved homolytically,[13,14] investigations have also been performed on the reactivity of the Fe^{III}(TPA)−$OOCH_3$ complex, thus providing insights on both the heterolytic and the homolytic cleavage mechanisms. The theoretical results acquired for the activity of

(10) (a) Chen, K.; Que, L., Jr. *J. Am. Chem. Soc.* **2001**, *123*, 6327−6337. (b) Zang, Y.; Kim, J.; Dong, Y.; Wilkinson, E. C.; Appelman, E. H.; Que, L., Jr. *J. Am. Chem. Soc.* **1997**, *119*, 4197−4205.
(11) Chen, K.; Costas, M.; Kim, J.; Tipton, A. K.; Que, L., Jr. *J. Am. Chem. Soc.* **2002**, *124*, 3026−3035.
(12) Chen, K.; Costas, M.; Que, L., Jr. *J. Chem. Soc., Dalton Trans.* **2002**, 672−679.
(13) MacFaul, P. A.; Ingold, K. U.; Wayner, D. D. M.; Que, L., Jr. *J. Am. Chem. Soc.* **1997**, *119*, 10594−10598.
(14) Ingold, K. U.; MacFaul, P. A. In *Biomimetic Oxidations Catalyzed by Transition Metal Complexes*; Meunier, B., Ed.; Imperial College Press: London, 2000; pp 45−89.
(15) Stevens, P. J.; Devlin, F. J.; Chablowski, C. F.; Frish, M. J. *J. Phys. Chem.* **1994**, *98*, 11623−11627.
(16) Becke, A. D. J. *Chem. Phys.* **1993**, *98*, 5648−5652; **1992**, *96*, 2155−2160; **1992**, *97*, 9173−9177.
(17) Lee, C.; Yang, W.; Parr, R. G. *Phys. Rev. B* **1988**, *37*, 785−789.
(18) *JAGUAR 4.0*; Schrödinger, Inc.: Portland, Oregon, 2000. See: Vacek, G.; Perry, J. K.; Langlois, J.-M. *Chem. Phys. Lett.* **1999**, *310*, 189−194.
(19) Frisch, M. J.; Trucks, G. W.; Schlegel, H. B.; Scuseria, G. E.; Robb, M. A.; Cheeseman, J. R.; Zakrzewski, V. G.; Montgomery, J. A., Jr.; Stratmann, R. E.; Burant, J. C.; Dapprich, S.; Millam, J. M.; Daniels, A. D.; Kudin, K. N.; Strain, M. C.; Farkas, O.; Tomasi, J.; Barone, V.; Cossi, M.; Cammi, R.; Mennucci, B.; Pomelli, C.; Adamo, C.; Clifford, S.; Ochterski, J.; Petersson, G. A.; Ayala, P. Y.; Cui, Q.; Morokuma, K.; Malick, D. K.; Rabuck, A. D.; Raghavachari, K.; Foresman, J. B.; Cioslowski, J.; Ortiz, J. V.; Stefanov, B. B.; Liu, G.; Liashenko, A.; Piskorz, P.; Komaromi, I.; Gomperts, R.; Martin, R. L.; Fox, D. J.; Keith, T.; Al-Laham, M. A.; Peng, C. Y.; Nanayakkara, A.; Gonzalez, C.; Challacombe, M.; Gill, P. M. W.; Johnson, B. G.; Chen, W.; Wong, M. W.; Andres, J. L.; Head-Gordon, M.; Replogle, E. S.; Pople, J. A. *Gaussian 98*; Gaussian, Inc.: Pittsburgh, PA, 1998.
(20) Hay, P. J.; Wadt, W. R. *J. Chem. Phys.* **1985**, *82*, 299−310.
(21) Barone, V.; Cossi, M. *J. Phys. Chem. A* **1998**, *102*, 1995−2001.
(22) Siegbahn, P. E. M. *J. Comput. Chem.* **2001**, *22*, 1634−1645.
(23) Siegbahn, P. E. M.; Blomberg, M. R. A. *Chem. Rev.* **2000**, *100*, 421−437.
(24) Curtiss, L. A.; Raghavachari, K.; Tucks, G. W.; Pople, J. A. *J. Chem. Phys.* **1991**, *94*, 7221−7230.
(25) Curtiss, L. A.; Raghavachari, K.; Redfern, P. C.; Pople, J. A. *J. Chem. Phys.* **1997**, *106*, 1063−1079.

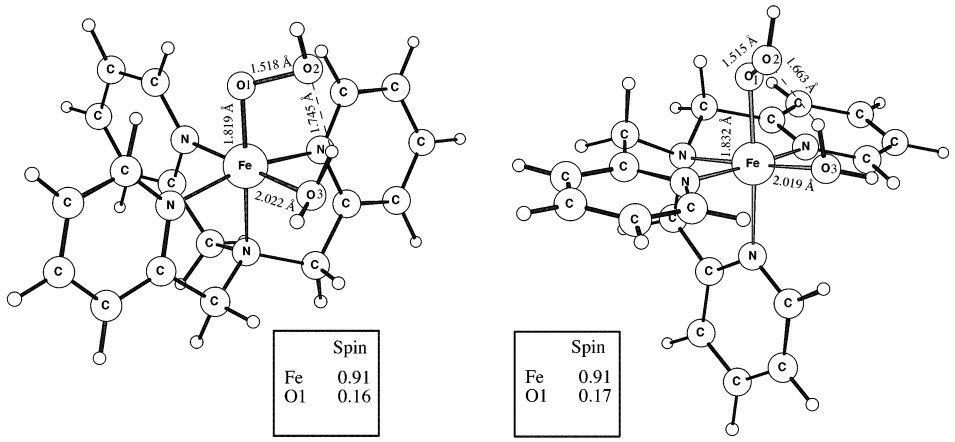

a. N_{amine}-complex **b. $N_{aromatic}$-complex**

Figure 2. The two possible doublet isomers for the reactant ($[Fe(TPA)(OOH)(H_2O)]^{2+}$). (a) N_{amine}-complex with OOH occupying the position trans to the to the sp^3 amine nitrogen; (b) $N_{aromatic}$-complex with OOH occupying the position trans to one of the aromatic nitrogen atoms.

the $Fe^{III}(TPA)-OOH$ complex are first presented, followed by a comparison between the reactivity properties of the two structurally similar complexes $Fe^{III}(TPA)-OOH$ and $Fe^{III}(TPA)-OOCH_3$.

III.a. Heterolytic O−O Bond Cleavage in the Hydroperoxide Complex. Calculations have been carried out for the case where the catalyst $Fe^{III}(TPA)-OOH$ in the stereospecific alkane hydroxylation is the simplest one of the various Fe(TPA) complexes, the one where no substituents are present in the pyridyl ring. Below, the geometric and electronic structures of the different intermediates are reported, together with the calculated energetics of the reaction path for the O−O bond heterolysis reaction.

The actual reactant can be formulated as a $[Fe(TPA)(OOH)]^{2+}$ complex, in which the octahedral coordination of iron is completed by a water molecule. Two different isomers are possible for this type of complex, as illustrated in Figure 2: the HOO^- ligand can occupy either the position trans to the sp^3 amine nitrogen (N_{amine}-complex) or the position trans to one of the aromatic nitrogen atoms ($N_{aromatic}$-complex). Different spin states arise from the specific configuration of the five d-electrons of Fe^{III}. For both the N_{amine}-complex and the $N_{aromatic}$-complex, the most stable state is found to be the low-spin state, characterized by one unpaired electron on the iron atom yielding a doublet multiplicity as is also found for the analogous [(Por)-$Fe^{III}-OOH$] species in cytochrome P450[6] and in cytochrome oxidase.[26,27] This theoretical result agrees with EPR measurements performed on the $Fe^{III}(TPA)-OOH$ intermediate trapped at −40 °C, where a species associated with a low-spin Fe^{III} center was identified.[28] The $Fe-N_{TPA}$ distances (1.96−2.03 Å) in the optimized structures of the two isomeric complexes are in reasonable agreement with the corresponding experimental ones measured for the $[Fe(5\text{-}Me_3TPA)(acac)]^{2+}$ system (1.93−1.99 Å).[10] The relatively short values reflect the small ionic radius of the iron center with a low-spin ground state, where in terms of ligand field theory a strong field is created by the ligands.

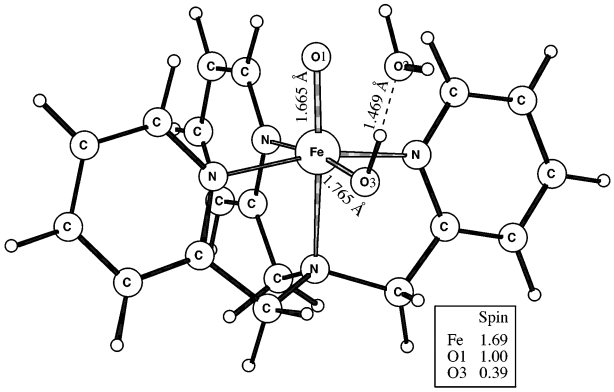

Figure 3. The *cis*-$HO-Fe^V$ complex formed by the O−O heterolytic cleavage.

The two isomers in their doublet electronic configuration are energetically similar, the N_{amine}-complex being more stable by only 2.6 kcal/mol than the $N_{aromatic}$-complex. For both isomers, the quartet state differs by 7.8 kcal/mol from the corresponding doublet ground state. Hereafter only the results concerning the lower energy isomer, that is, the N_{amine}-complex, will be presented, because, for the whole chemical reaction under consideration, the $N_{aromatic}$-complex gives very similar but slightly higher energies, with an O−O bond cleavage transition state occurring a few kcal/mol higher than that of the N_{amine}-complex.

According to the proposed mechanism, the product of the O−O bond cleavage is postulated to be an $Fe^V{=}O$ complex (see Figure 1). The ground state of the *cis*-$HO-Fe^V{=}O$ product is computed to be a quartet, and the optimized geometry is shown in Figure 3. The overall O−O bond cleavage reaction was found to be endergonic by 5.1 kcal/mol.

Because the product of the O−O bond heterolysis has a quartet ground state and the reactant has a doublet ground state, somewhere along the reaction path a spin-forbidden transition has to take place, which should be favored by the large spin−orbit coupling at the iron center. Because of the accessibility of the quartet state of the $Fe^{III}(TPA)-OOH$ reactant, lying only 7.8 kcal/mol higher in energy than the doublet state, the spin-crossing could, in principle, occur before or after the transition state is passed. The calculations show that the transition state corresponding to the O−O bond cleavage on the quartet

(26) Blomberg, M. R. A.; Siegbahn, P. E. M.; Babcock, G. T.; Wikström, M. *J. Am. Chem. Soc.* **2000**, *122*, 12848−12858.
(27) Blomberg, M. R. A.; Siegbahn, P. E. M.; Babcock, G. T.; Wikström, M. *J. Inorg. Biochem.* **2000**, *80*, 261−269.
(28) Kim, C.; Chen, K.; Kim, J.; Que, L., Jr. *J. Am. Chem. Soc.* **1997**, *119*, 5964−5965.

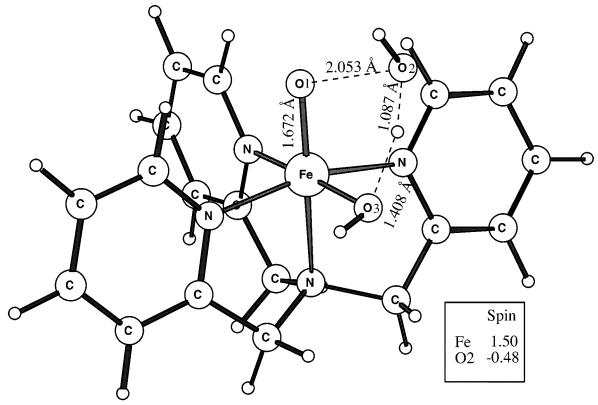

Figure 4. The transition state on the doublet potential energy surface leading to the O−O bond cleavage in the Fe^{III}(TPA)−OOH complex.

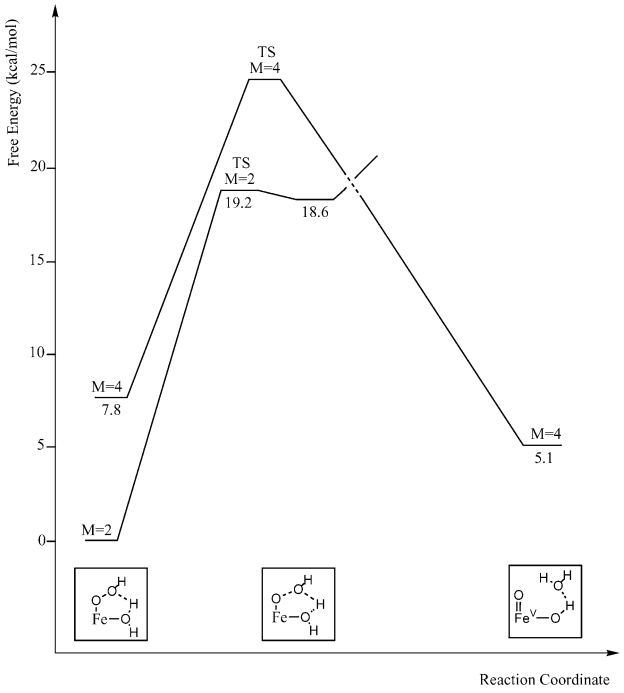

Figure 5. Reaction paths for the heterolytic O−O bond cleavage promoted by the Fe^{III}(TPA)−OOH catalyst. The spin multiplicity *M* of the two potential energy surfaces is indicated.

potential energy surface is located at a much higher energy than the corresponding transition state on the doublet surface, and an early spin-crossing can thus be excluded. The doublet transition state gives a barrier of 19.2 kcal/mol, and the optimized structure is reported in Figure 4 together with the most important spin populations. Both the structure and the spin-populations are strikingly similar to the transition state previously suggested for O−O bond formation in photosystem II.[29,30] As further discussed below, the spin-crossing is estimated to take place rather close to the doublet transition state as indicated in the calculated potential energy surface for the O−O heterolytic cleavage summarized in Figure 5. The computed energetics for this reaction path indicate that the proposed mechanism of Figure 1 is feasible.

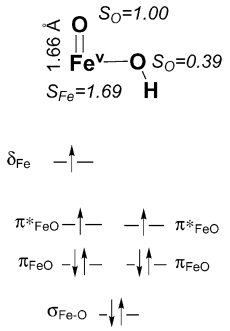

Figure 6. Qualitative orbital picture describing the electronic structure of the Fe^V═O intermediate. The computed spin distribution and Fe−O bond length are also reported.

The reduction of hydrogen peroxide to water requires two electrons. In the mechanism shown in Figure 1, both of these electrons are supplied by the metal center, with a resulting Fe^V oxidation state in the iron-oxo product. On the basis of the molecular orbital picture, which will be discussed below, two unpaired electrons are expected to be localized on iron in the Fe^V═O complex. In the calculated spin populations given in Figure 3, a spin of almost 2 (1.69) is indeed found on the metal, thus supporting the Fe^V oxidation state. As a comparison, it can be noted that the O−O bond cleavage in cytochrome P450 and peroxidases leads to an iron-oxo product with an Fe^{IV} oxidation state and a porphyrin radical ($[(Por^{\bullet})Fe^{IV}{=}O]^{+1}$), commonly referred to as Compound I. The main electronic difference between Compound I and the Fe^V═O product of the present reaction is that, while in Compound I the porphyrin ligand is able to provide one of the electrons needed for the oxygen reduction, in the TPA catalyst both electrons are withdrawn from the iron atom itself. Despite several attempts, no ferryl-oxo product with substantial spin density on the TPA ligand (i.e., a TPA ferryl-oxo compound analogous to Compound I with a porphyrin radical) could be found in our calculations.

According to the molecular orbital picture describing the Fe−O double bond,[31,32] two ferromagnetically coupled unpaired electrons occupy two degenerate π^* orbitals in Compound I as well as in the biomimetic iron-oxo product, yielding a spin population of about 1 on both the metal and the oxo-group. In Compound I, the additional unpaired electron, localized on the porphyrin ligand, is antiferromagnetically coupled to the two unpaired π^* electrons, with a resulting doublet ground state. In contrast, the additional unpaired electron in the (TPA)Fe^V═O product is mainly localized on iron and must thus be ferromagnetically coupled to the other unpaired electrons in the two degenerate π^*_{FeO} orbitals, to lower the total energy by maximizing the exchange interaction. This consequently yields a spin of about 2 on iron and a high-spin coupled quartet ground state for the product. A qualitative orbital picture describing the electronic structure of the (TPA)Fe^V═O intermediate is reported in Figure 6.

As can be noted in Figure 3, the spin on the iron atom is not 2 but rather 1.69. Some unpaired spin density is, in fact, partly delocalized on the hydroxyl ligand, with a spin of 0.39 on

(29) Siegbahn, P. E. M.; Crabtree, R. H. *J. Am. Chem. Soc.* **1999**, *121*, 117−127.
(30) Siegbahn, P. E. M.; Blomberg, M. R. A. In *Theoretical Chemistry − Processes and Properties of Biological Systems*; Eriksson, L. A., Ed.; Elsevier: Amsterdam, 2001; pp 95−137.
(31) Yoshizawa, K.; Shiota, Y.; Yamabe, T. *J. Am. Chem. Soc.* **1998**, *120*, 564−572.
(32) Shaik, S.; Filatov, M.; Schröder, D.; Schwarz, H. *Chem.-Eur. J.* **1998**, *4*, 193−199.

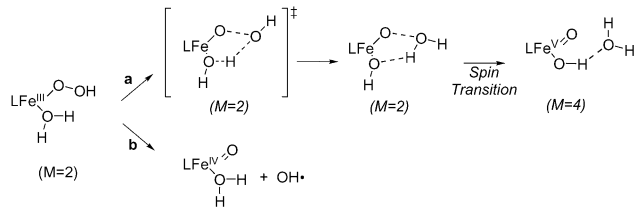

Figure 7. Heterolytic (a) and homolytic (b) pathways for the O−O bond cleavage in the Fe(TPA) catalyst. The total multiplicity *M* of the system during the heterolysis is also shown for clarity.

oxygen. The rather high spin population on the hydroxyl ligand is probably one reason that the $Fe^{V}-OH$ bond is as short as 1.76 Å. A comparison between the structures in Figures 3 and 4 shows that the hydrogen bonding between the hydroxyl ligand and the newly formed water molecule has to rearrange from the transition state structure to the product, as also shown in pathway a of Figure 7, where the mechanism for the O−O heterolysis is schematically summarized. This hydrogen bond rearrangement will be further discussed below. It is clear that with the loss of almost one-half of an electron from the OH ligand in the product, the hydrogen bond formed with the hydroxyl ligand as proton donor rather than as proton acceptor is energetically favorable, and the short hydrogen bonding distance of 1.47 Å indicates a strong hydrogen bond.

As mentioned above, the O−O bond cleavage must involve a spin-crossing, which makes the full investigation of this reaction mechanism quite complicated. By exploring the doublet surface, a transition state was located with an imaginary frequency (184 cm^{-1}) mainly connected with the O−H stretching toward the formation of the new water molecule (see Figure 4, where the atomic labels used below are given). After passing the transition state, a very shallow minimum is immediately found, having an energy (18.6 kcal/mol), structure, and spin distribution very similar to those of the transition state. The spin distribution in this region of the doublet potential energy surface can be rationalized in terms of the changes in the electronic structure leading finally to the orbital structure for the Fe═O double bond depicted in Figure 6. The O−O cleavage starts with the excitation of one β electron into the O1−O2 antibonding σ^* orbital,[33,34] accounting thus for the 0.48 β spin on O2 (see Figure 4). The remaining O1−O2 bonding of effectively one σ electron explains why there is a minimum in this region with a relatively long distance of 2 Å between the two oxygen atoms. A very similar minimum is, in fact, found also in the lowest excited state of hydrogen peroxide.[35] The net increase of α spin observed on the metal (from 0.91 in the reactant to 1.5 in the transition state) reflects a β electron depletion on iron, due to the excitation of the β electron from an Fe−O1 π^* orbital and the beginning of the Fe═O double bond formation, as also indicated by the short Fe−O1 distance of 1.67 Å.

To complete the O−O heterolytic cleavage, still another electron has to be transferred into the O1−O2 σ^* orbital, which finally removes both the remaining spin on the newly formed water molecule and any bonding between O1 and O2. As discussed above in relation to the electronic structure of the

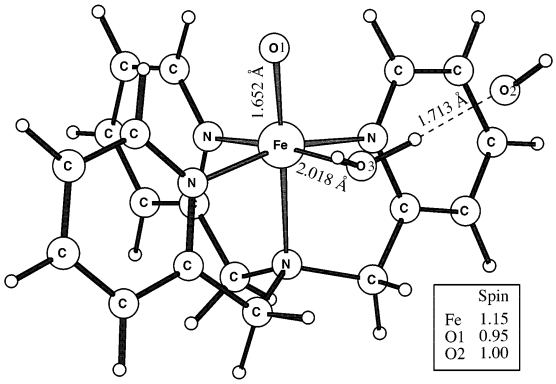

Figure 8. The Fe^{IV}═O product following the O−O homolytic bond cleavage and the release of the OH• radical in the Fe^{III}(TPA)−OOH complex.

product, this electron is mainly supplied by iron. The unpaired electron left on iron has to be ferromagnetically coupled to the other unpaired electrons to reach an energetically favorable iron-oxo compound. A spin-crossing is thus needed together with the electron transfer. Another requirement also has to be fulfilled for this chemical transformation to occur, and that is a reorganization of the hydrogen bonding, where the newly formed water molecule acts as proton acceptor rather than as proton donor (see pathway a of Figure 7). It can finally be added that the present electronic structure picture of the O−O bond cleavage has large similarities to the one previously found in cytochrome oxidase.[36]

The details of the hydrogen bonding rearrangement that evolves in the formation of the final iron-oxo product turned out to be quite complicated. A careful inspection of both the doublet potential energy surface, where the OH ligand acts as proton acceptor, and the quartet surface, where OH, on the contrary, is a proton donor, indicates that a curve crossing occurs between the two surfaces shortly after the transition state is passed. It is possible that this curve crossing occurs at a slightly higher energy than the transition state described above. At present, there are no methods capable of locating such a spin-crossing for the present size of the model system. Furthermore, a correct and complete representation of the change of hydrogen bonding probably requires an even larger model including the short-range action of some solvent molecules, which may play a role to promote this rearrangement. Although it is not possible from the chosen model system to fully derive the reaction path that leads to the product, the collected information is still representative of the chemical transformation depicted in Figure 1. In fact, both potential energy surfaces in the curve crossing region are found to be very shallow, supporting the conclusion that the main characteristics (energetics and relevant bond distances) of the optimized transition state reflect the actual transition state for the O−O bond heterolytic cleavage in the biomimetic non-heme iron catalyst.

III.b. Homolytic O−O Bond Cleavage in the Hydroperoxide Complex. The homolytic cleavage of the O−O bond (pathway b of Figure 7), leading to an OH• radical and an Fe^{IV}═O complex (see Figure 8), has also been considered, and the resulting potential energy surface is illustrated in Figure 9, where the heterolytic pathway is included for comparison.

The ground state of the Fe^{IV}═O complex is a triplet, with spin populations of 1.15 on iron and 0.95 on the oxo-oxygen.

(33) Lehnert, N.; Ho, R. Y. N.; Que, L., Jr.; Solomon, E. I. *J. Am. Chem. Soc.* **2001**, *123*, 8271−8290.
(34) Lehnert, N.; Ho, R. Y. N.; Que, L., Jr.; Solomon, E. I. *J. Am. Chem. Soc.* **2001**, *123*, 12802−12816.
(35) Bassan, A.; Blomberg, M. R. A.; Siegbahn, P. E. M.; Roos, B. O., to be published.
(36) Blomberg, M. R. A.; Siegbahn, P. E. M.; Wikström, M., to be published.

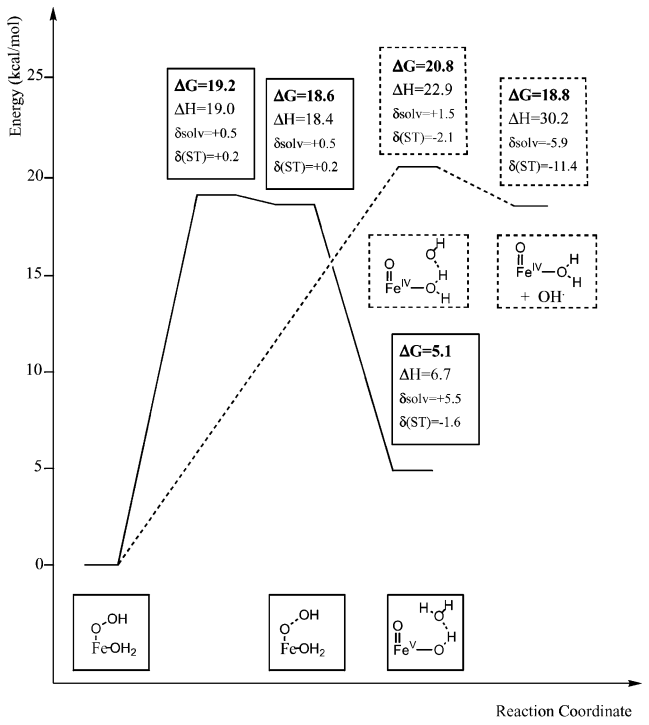

Figure 9. Potential energy surfaces for O−O homolysis (dashed line) and heterolysis (solid line) promoted by the Fe^{III}(TPA)−OOH catalyst. Free energies (ΔG) include solvent corrections (δsolv) and entropy effects (δ(ST)) at 298.15 K.

For the product shown in Figure 8, two nearly degenerate spin states, a doublet and a quartet, arise from the different couplings between the two unpaired electrons located on the iron-oxo complex and the unpaired electron located on the OH· radical.

The O−O homolysis leading to the product shown in Figure 8 is an uphill process without any transition state. This process is computed to be endergonic by 20.8 kcal/mol, and thus has an energy barrier slightly higher than that for O−O heterolysis with a barrier of 19.2 kcal/mol. However, in the product depicted in Figure 8, the OH· radical is not strictly free; it is, in fact, trapped by a hydrogen bond with the water ligand, and it is also held in the proximity of the metal complex by a strong electrostatic attraction from the high-valent iron center. To create a completely free hydroxyl radical, the distance between iron and OH· needs to be increased, which consequently leads to a loss of hydrogen bonding and electrostatic energy and an increase of entropy. The binding energy in the gas phase of the OH· radical to the iron complex was evaluated to be 14.7 kcal/mol, which is surprisingly large. However, the large entropy effect, 11.4 kcal/mol, together with an unusually large solvent effect of 5.9 kcal/mol for the free radical, more than cancels the high binding energy of the hydrogen-bonded system. Therefore, when the entropy and the solvent are considered, the free OH· becomes slightly more stable than the hydrogen-bonded structure, with endergonicities of 18.8 and 20.8 kcal/mol, respectively. The large solvent correction is related to the presence of the high-valent metal ion and the concomitant increase of the dipole moment as estimated for the bare iron complex with and without the hydrogen-bonded OH·. From the product in Figure 8, a further oxidation of Fe^{IV} to Fe^{V} could, in principle, take place through a hydrogen atom transfer from the water ligand to the hydrogen-bonded OH· radical. This process was investigated, but it is ruled out by a computed activation energy which is too high.

III.c. Comparison between the O−O Heterolysis and the O−O Homolysis in the Hydroperoxide Complex. The results presented above show that the O−O bond can be cleaved both heterolytically and homolytically with the subsequent formation of different products. The formation of the Fe^{V}═O intermediate and a water molecule, as illustrated in Figure 3, follows O−O heterolysis, whereas the product of the O−O homolysis is the OH· radical bonded to the Fe^{IV}═O intermediate, shown in Figure 8. These results alone cannot definitively predict which of the two different O−O cleavage pathways is actually preferred by the Fe^{III}(TPA)−OOH intermediate, because both reactions are computed endergonic and have barriers of comparable size. One argument against the homolytic pathway should be mentioned at this point. The estimated free energy barrier for the homolytic cleavage is probably not the highest point on the free energy surface. The further release of the OH· radical from the hydrogen-bonded system, having a free energy of 20.8 kcal/mol, is connected with large changes involving decreasing enthalpy and increasing entropy and solvent effects. Even if these effects cancel each other for the totally free radical, it is more than likely that there will be an additional barrier for this process.

To get more detailed information on which pathway is followed in the hydroxylation reaction with alkanes studied experimentally,[10] the next step in this process can also be considered. As a first step in this direction, the hydrogen atom abstraction from cyclohexane by a free OH· was studied and was found to occur without any considerable enthalpy barrier. However, when the entropy effects are added, the free energy barrier for this process becomes 5.0 kcal/mol. Because the starting point for the hydrogen abstraction by the OH· is already 18.8 kcal/mol higher than that of the Fe(TPA)−OOH reactant, the total barrier for the homolytic pathway towards hydroxylation is 23.8 kcal/mol. The heterolytic process with a free energy barrier of 19.2 kcal/mol is thus favored by 4.6 kcal/mol. For a hydroxylation process following the heterolytic pathway, much higher barriers for the following steps after the O−O cleavage can be afforded, because the product of the O−O cleavage is 14.1 kcal/mol lower than the O−O cleavage barrier for this pathway.

A preliminary investigation on the activation energy required for alkane hydroxylation by the Fe^{V}═O species lends further support to the heterolytic pathway. Hydroxylation of methane by the high-valent iron-oxo species has been probed according to the rebound mechanism, which involves, first, a hydrogen atom abstraction by the high-valent iron-oxo species and, second, a radical rebound leading to the alcohol product. The hydrogen atom abstraction is found to occur on the quartet potential energy surface through a transition state, which has been estimated to lie about 14 kcal/mol higher in energy than the starting metal-based oxidant, the Fe^{V}═O intermediate plus methane. Zero-point vibrational effects, which have not been calculated yet, can be estimated to lower this barrier height by about 5 kcal/mol, a value which is taken from similar calculations on methane monooxygenases (MMO).[37] Hydroxylation of methane by the oxo-ferryl intermediate continues with a spin

(37) Siegbahn, P. E. M.; Crabtree, R. H. *J. Am. Chem. Soc.* **1997**, *119*, 3103−3113.

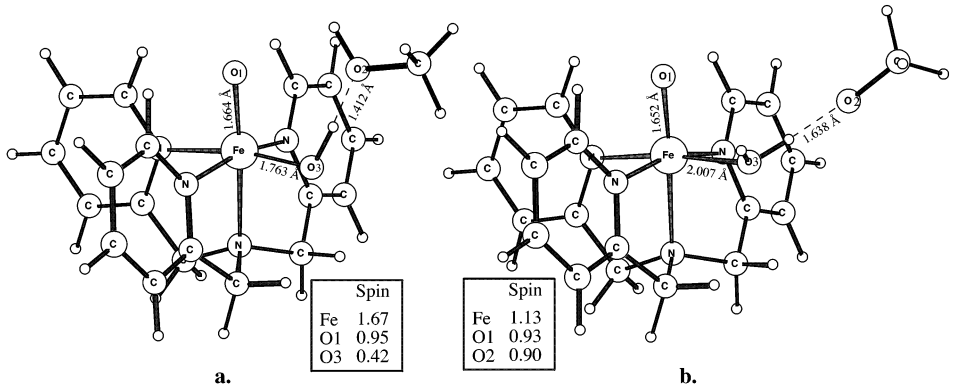

Figure 10. Products of the O−O cleavage for the $HOOCH_3$ oxidant: (a) Fe^{V}═O formed by O−O heterolysis; (b) Fe^{IV}═O formed by O−O homolysis.

transition to the doublet potential energy surface, where the rebound step is computed to occur almost without any barrier in agreement with the theoretical findings by Ogliaro et al.[38] Because the C−H bond strength of cyclohexane is 94.1 kcal/mol and that of methane is 102.0 kcal/mol, at least 5 kcal/mol of this 8 kcal/mol difference can be expected to decrease the barrier of the hydrogen atom abstraction from cyclohexane by the oxo-ferryl species. The zero-point effects together with the lower C−H bond strength in cyclohexane lead to an expected barrier of about 4 kcal/mol. If this energy is added to the energy of 5.1 kcal/mol for the Fe^{V}═O species, one arrives at an energy of about 9 kcal/mol to be compared to 19.2 kcal/mol for the O−O bond activation. It can therefore safely be concluded that the cyclohexane hydroxylation should not be rate-limiting for the heterolysis pathway. In light of the previously discussed objections against the homolytic pathway, the heterolysis thus appears as the preferred route for the O−O cleavage in the (TPA) catalyst.

The present calculations thus give a rationalization for why the OH· radical mechanism in the alkane hydroxylation by Fe(TPA) is not experimentally observed with hydrogen peroxide as oxidant. Only stereospecific hydroxylation is seen, following the Fe^{V} pathway. A detailed investigation on this pathway all the way to the hydroxylated product has not been completed yet.

III.d. Homolytic O−O Bond Cleavage in the Alkylperoxide Complex. It is interesting to note that with alkyl hydroperoxides, Fe−TPA catalyzed hydroxylation does not lead to stereospecific products in contrast to the case of hydrogen peroxide.[13] To increase the understanding of the difference between the two systems, some calculations were done also for an $HOOCH_3$ oxidant. The results show that for alkylperoxides, the product of the O−O bond homolysis is significantly more stable than it is for hydrogen peroxide. In fact, for alkylperoxides the products for O−O bond homolysis and heterolysis are almost degenerate with computed endergonicities of 9.7 and 9.1 kcal/mol, respectively. Figure 10 reports the structural details for the corresponding Fe^{IV}═O and Fe^{V}═O products, which are quite similar to the corresponding products of the O−O cleavage in Fe^{III}(TPA)−OOH. For the alkylperoxide complex, the activation energy for the heterolytic reaction path is shown by the calculations to be very similar to the analogous hydroperoxide case and is not discussed further here.

The homolytic cleavage is found to pass through a transition state with a free energy of 16.3 kcal/mol, which occurs at an O−O distance of 2 Å as shown in the structure reported in Figure 11. The immediate product of the O−O homolysis is again a hydrogen-bonded radical, which, when released, slightly lowers the free energy of the final homolytic product to 8.9 kcal/mol. The details of the energetics for the homolytic cleavage are reported in Figure 12, where a comparison with the corresponding homolytic reaction with hydrogen peroxide as oxidant is also highlighted. The computed potential energy surface indicates that the increased stability of the alkoxy radical makes the homolysis efficiently competitive with the heterolytic alternative when $HOOCH_3$ is used as oxidant.

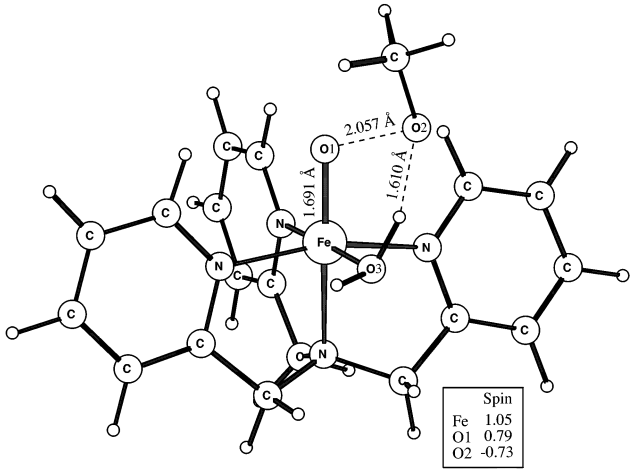

Figure 11. The transition state on the doublet potential energy surface leading to the O−O bond cleavage for the Fe^{III}(TPA)−$OOCH_3$ complex.

The general picture obtained for the homolytic cleavage of the alkyl peroxide is in good agreement with the previous theoretical investigation performed by Lehnert et al.[33,34] on a similar system. They found a maximum in the potential energy surface of the O−O homolysis at a distance similar to that of the present transition state and with a similar relative energy. They also computed large entropic and solvent effects when the methoxy radical becomes free, with values very similar to the present ones, which are given in Figure 12. One difference in the results between the previous and the present theoretical study is that no significant transition state was found by Lehnert et al., while, in the present study, a pronounced transition state is localized. Another difference is that they computed the homolytic O−O cleavage step to be thermoneutral, while, in the present study, the reaction is found to be endergonic by about 9 kcal/mol. None of these differences have any significant effects on the general conclusions drawn, and they are most

(38) Ogliaro, F.; Harris, N.; Cohen, S.; Filatov, M.; de Visser, S. P.; Shaik, S. *J. Am. Chem. Soc.* **2000**, *122*, 8977−8989.

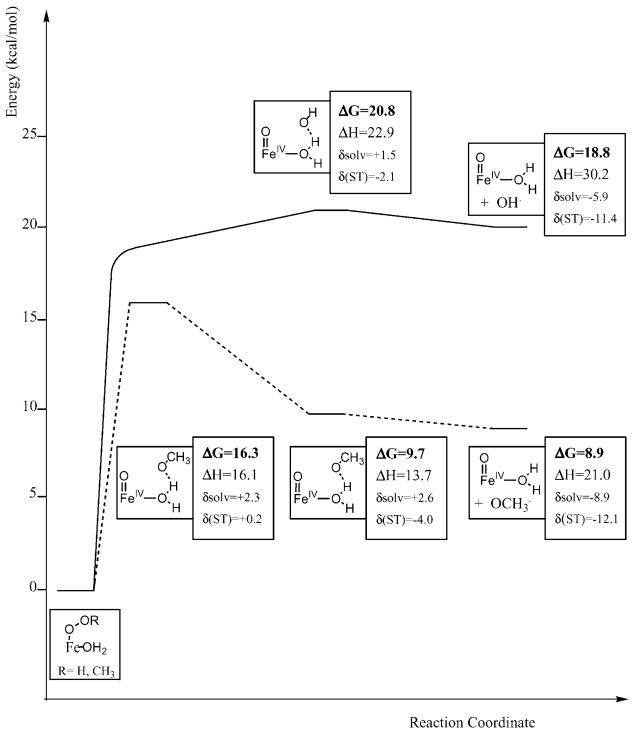

Figure 12. Potential energy surfaces for O−O homolysis promoted by the catalytic activity of Fe^{III}(TPA)−OOH (solid line) and Fe^{III}(TPA)−$OOCH_3$ (dashed line). Free energies (ΔG) include solvent corrections (δsolv) and entropy effects (δ(ST)) at 298 K.

likely explained by differences in the model systems used for the investigations. The most important difference is probably that a hydroxyl ligand was used in the previous study instead of a water ligand in the present model. Also, Lehnert et al. used ammonia ligands instead of the full TPA molecule, and a *tert*-butylperoxo group rather than the methyl peroxo group, as used in the present investigation.

For the alkylperoxide intermediate, the accessibility of the homolytic path, which seems to be precluded for the hydroperoxide case discussed before, is due to the different O−O bond strengths computed for H_2O_2 and CH_3O_2H,[35] of 51.9 and 43.9 kcal/mol, respectively, reflecting a better delocalization of the radical in the methoxy case. The 8.0 kcal/mol difference between the two bond energies is comparable to the 9.9 kcal/mol difference between the relative energies of the two radical products, 18.8 kcal/mol for the O−O homolysis of HOOH and 8.9 for the O−O homolysis of $HOOCH_3$. Therefore, the strength of the O−O bond governs the reaction path adopted in the catalysis by Fe(TPA) complexes. Although homolytic and heterolytic O−O cleavage occur with similar energy barriers, the homolytic path is prevented by the high relative energy of the product for the Fe^{III}(TPA)−OOH catalyst. Stereospecific hydroxylation is then carried out by the Fe^{V}═O intermediate. On the other hand, for alkylperoxides, the radical produced is much more stable, by 10 kcal/mol, and can therefore be released to then react with the alkanes leading to nonstereospecific products. Because the actual oxidant in the alkylperoxide experiments was *tert*-butyl peroxide and not methyl peroxide, a calculation was finally done for the O−O bond strength in the *tert*-butyl case. The result is 43.8 kcal/mol, almost the same as that in CH_3O_2H, and the two oxidants are therefore expected to behave quite similarly.

IV. Conclusions

Calculations have been performed on the Fe(TPA) catalyst to shed light on the reactivity of these inorganic complexes, which have been found experimentally to be capable of stereospecific alkane hydroxylation when hydrogen peroxide is used as oxidant.[10] Highly stereoselective olefin epoxidation and olefin *cis*-dihydroxylation can be catalyzed as well.[11,12] The active species in catalysis is proposed to be Fe^{III}(TPA)−OOH, where the cleavage of the O−O bond promoted by a water molecule ligated to the metal center may lead to two different products. A homolytic cleavage of the O−O bond leads to Fe^{IV}═O and an OH· radical, which would imply the involvement of the nonselective OH· radical oxidant in the subsequent oxidations, while a heterolytic bond cleavage is responsible for the formation of the high-valent iron-oxo species Fe^{V}═O, a selective oxidant which can carry out stereospecific alkane hydroxylation. Although the homolytic and the heterolytic pathways are computed to occur with similar energy barriers, they differ significantly in the relative energy of the iron-oxo product of the O−O cleavage. The Fe^{IV}═O plus OH· radical product of O−O homolysis is too endergonic to allow the subsequent reaction between the oxidant and the hydrocarbon. On the other hand, the Fe^{V}═O product of the O−O heterolytic pathway is formed with an endergonicity of only 5.1 kcal/mol, and this product will lead to a stereospecific alkane hydroxylation in the next step.

Parallel calculations on the analogous Fe^{III}(TPA)−OOR species lend confidence to our mechanistic conclusions. Experimentally, the Fe(TPA)/ROOH combination has been shown to oxidize alkanes, generating long-lived alkyl radicals, which result in loss of stereochemistry.[13] These results implicate an alkoxy radical oxidant, presumably derived from O−O homolysis. Unlike the hydroperoxide case, the calculations show that the two intermediates produced by O−O homolysis and heterolysis in the alkylperoxide case are almost degenerate at an energy which is low enough to allow the hydrocarbon oxidation to occur. The calculations further give a lower barrier for the homolytic path, indicating that the alkoxy radical should be the main oxidant, in agreement with the observed loss of stereochemistry. However, because experiments showed that the chemistry with ROOH as oxidant exclusively involves O−O homolysis,[13] the computed energetic preference for the homolytic path is somewhat too small. An error of the B3LYP method of a few kcal/mol is what must be accepted. The origin of the difference in the results for the peroxide and the alkylperoxide oxidants is that the alkoxy radical is 8.0 kcal/mol more stable than the hydroxyl radical.

In the present work, the electronic structure has also been characterized for the product of the heterolytic cleavage of the O−O bond in Fe^{III}−OOH, demonstrating that it is best described as a high-valent Fe^{V}═O compound, where two electrons have been taken from the mononuclear Fe^{III} center. The Fe^{V}═O intermediate can be compared to the analogous species $[(Por\cdot)Fe^{IV}{=}O]^{+1}$ in cytochrome P450 and $Fe_2^{IV}(\mu\text{-}O)_2$ in methane monooxygenase, where instead the oxidizing equivalents implied by the formally Fe^{V} state are delocalized over two redox-active centers (i.e., iron and the porphyrin ring in P450 and two iron centers in methane monooxygenase).

JA026488G